

Journal Name

ARTICLE

Combined DFT and experimental study on nucleation mechanism of NiO nanodots on graphene

Yulan Lu,^{a,b} Lijun Su,^{b,c} Jing Qi,^{*a} Shulai Lei,^{*b} Bao Liu,^{b,c} Qi Zang,^d Siqi Shi,^e and Xingbin Yan^b

- a. School of Physical Science and Technology, Lanzhou University, Lanzhou, 730000, China
- b. Laboratory of Clean Energy Chemistry and Materials, State Key Laboratory of Solid Lubrication, Lanzhou Institute of Chemical Physics, Chinese Academy of Sciences, Lanzhou, 730000, P. R. China
- c. University of Chinese Academy of Sciences, Beijing 100039, P. R. China
- d. School of Materials Science and Engineering, Northwest Normal University, Lanzhou, 730070, China
- e. School of Materials Science and Engineering, Shanghai University, Shanghai, 200444, P. R. China

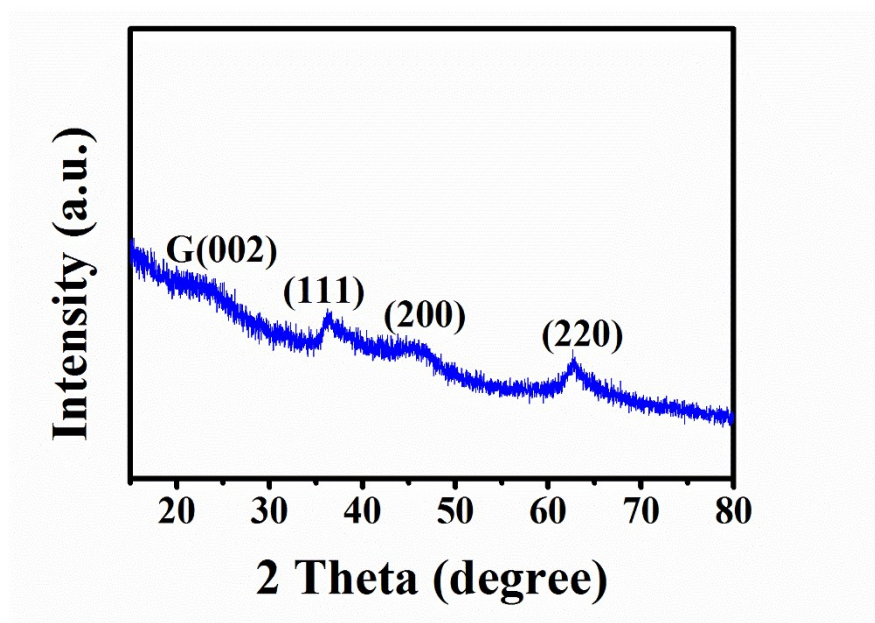


Fig. S1 X-ray diffraction (XRD) patterns of NiO NDs@rGO. The three main peaks can be indexed to the NiO phase (space group Fm-3m, JCPDS 47-1049). And the weak and broad peak at 2θ around 24° refers to disorderedly stacked graphene sheets, demonstrating the presence of NiO NDs and rGO.

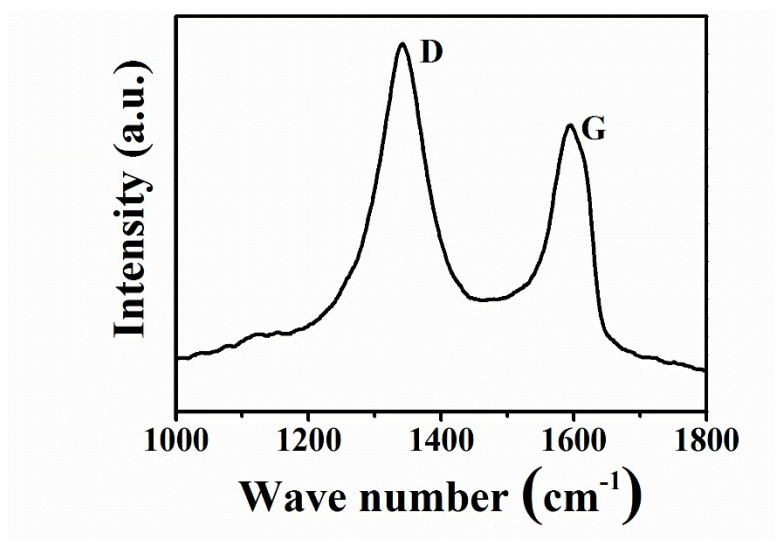


Fig. S2 The Raman spectra of NiO NDs@rGO composite. It can be seen that there are obvious characteristic peaks of disorder-induced D band and order-induced G band at 1350 and 1580 cm⁻¹, respectively.¹ Moreover, the intensity ratio of the D peak over the G peak (I_D/I_G) is 1.3, indicating that there are many defects on the surface of the rGO, such as vacancies², topological defects³ and oxygen-containing functional groups^{4,5}.

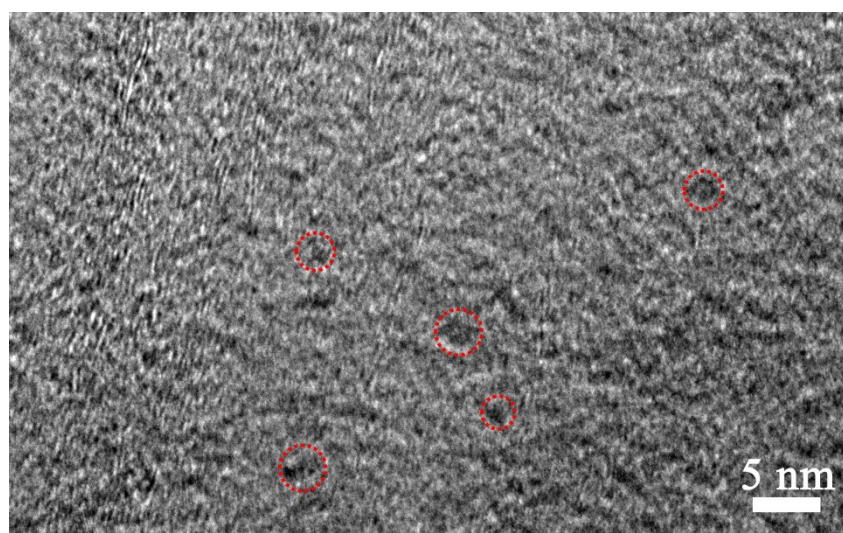


Fig. S3 TEM images of NiO NDs@rGO composite. The red circles indicate some NiO NDs.

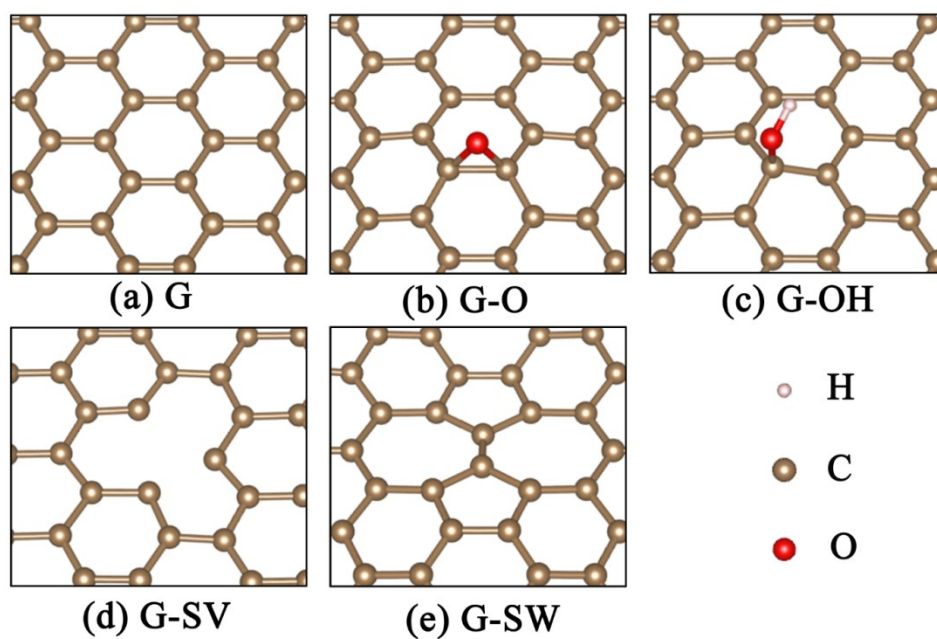


Fig. S4 Relaxed lattice structure of perfect graphene and graphene loaded with four different kinds of point defects.

Table. S1 The Elemental composition of various atoms present on the NiO NDs@rGO composites surface characterized by XPS.

Name	C 1s	N 1s	Ni 2p	O 1s
Atomic %	67.25	3.72	6.4	22.63

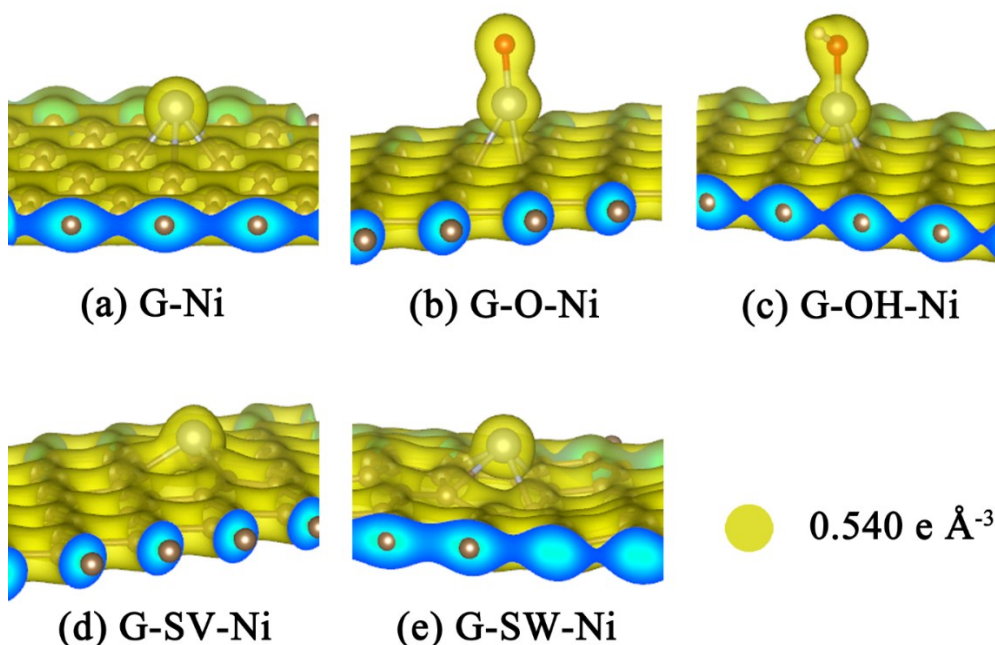


Fig. S5 The valence charge density distribution diagrams. For G-Ni, there is only a weak electron cloud overlap between the Ni and graphene. In contrast, for G-O-Ni and G-OH-Ni, there is a considerable overlap between Ni atom and neighbouring C atoms. In the case of the G-SV-Ni, it is observed that the strongest overlap locates on Ni and three dangling C bonds. The larger the overlapping area of charge density, the stronger the covalent interaction, this is consistent with absorption energy calculation results.

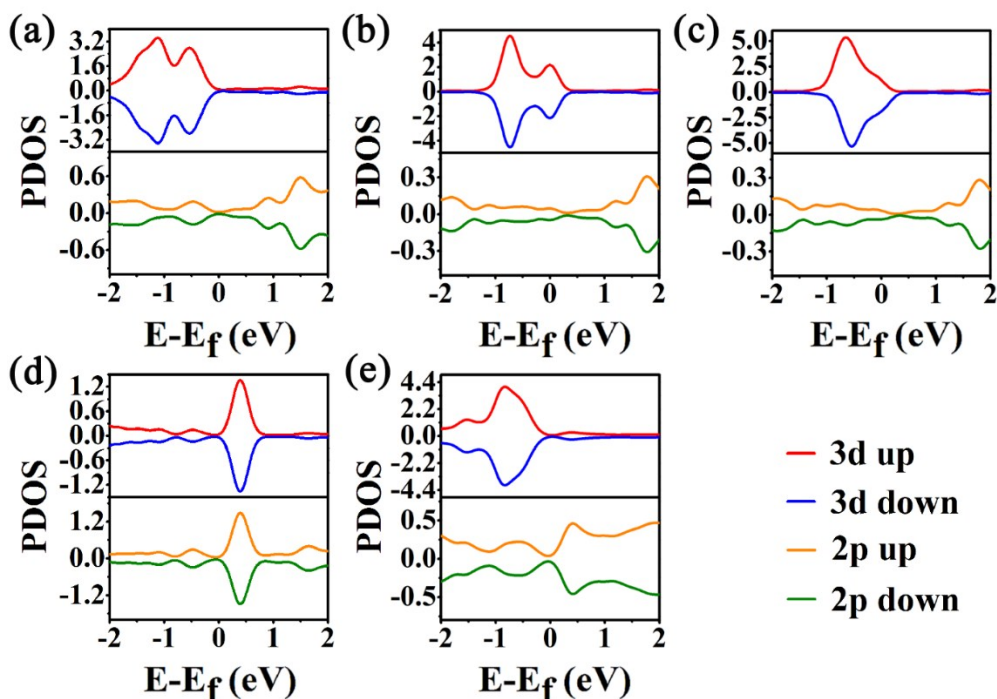


Fig. S6 The partial densities of states (PDOS) of Ni 3d orbital and C 2p orbital at the (a) G-Ni, (b) G-O-Ni, (c) G-OH-Ni, (d) G-SV-Ni, and (e) G-SW-Ni interface. It shows that the spin states of the 3d orbital of the Ni atom and the 2p orbital of the neighbouring C atoms are near the interface. The Ni 3d orbital partially hybridizes with the adjacent C 2p orbital, which is a typical Ni-C covalent bond characterization. In particular, due to the orbital of Ni 3d orbital partially hybridized with the dangling C bonds to form Ni-C bonds, in which the interaction is the strongest, the PDOS of adjacent C atoms match consistently with and Ni 3d orbital in G-SV-Ni.

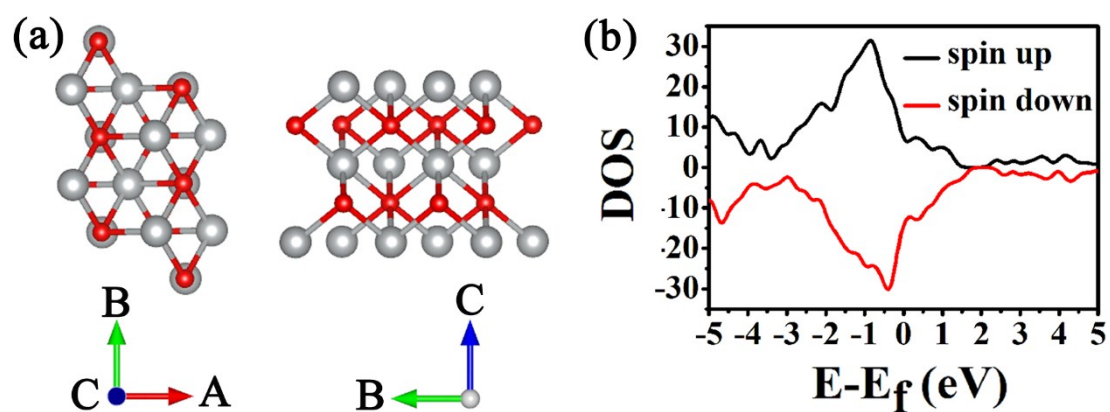


Fig. S7 (a) The structures in top and side view and (b) the densities of states (DOS) of NiO cluster.

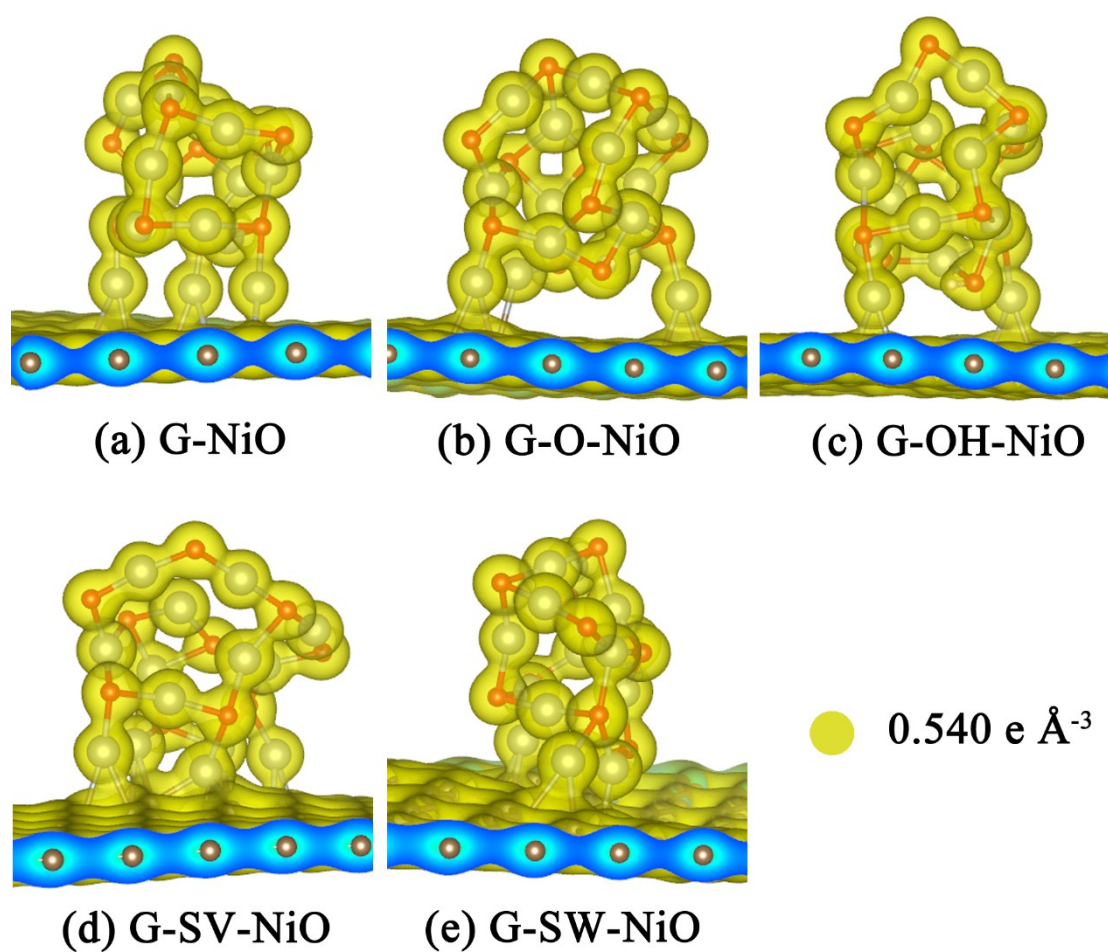


Fig. S8 The valence electron density for (a) G-NiO, (b) G-O-NiO, (c) G-OH-NiO, (d) G-SV-NiO, (e) G-SW-NiO.

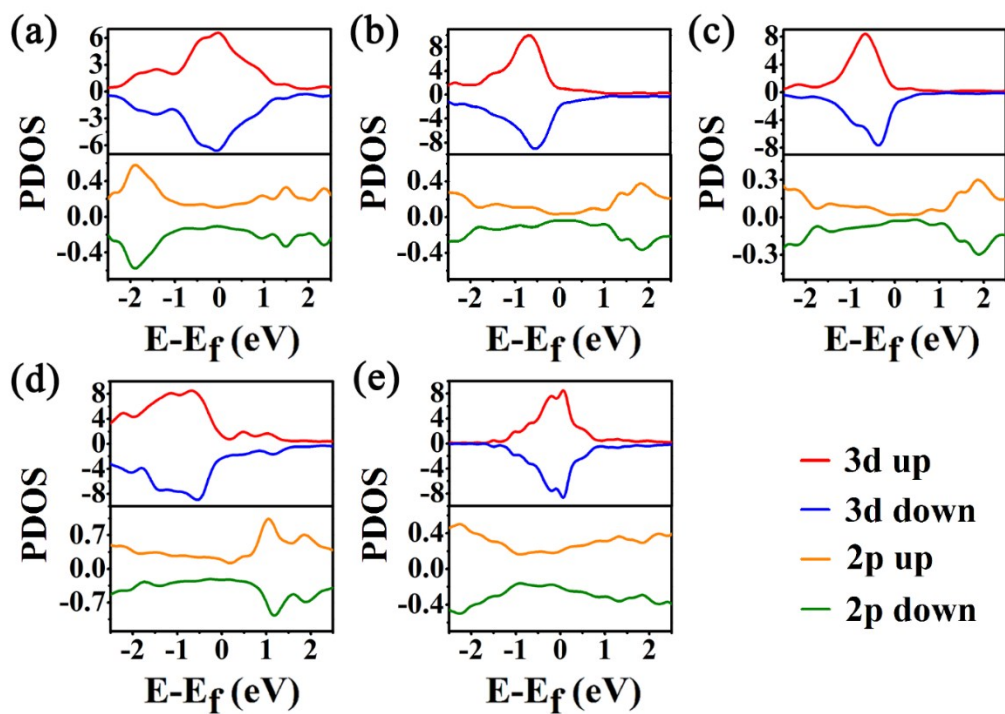


Fig. S9 The PDOS of Ni 3d orbital and C 2p orbital at the (a) G-NiO, (b) G-O-NiO, (c) G-OH-NiO, (d) G-SV-NiO, and (e) G-SW-NiO interface. PDOS is taken to highlight the effects of the interfacial interaction. Similar to a system that adsorbs one Ni atom, the 3d orbital of the Ni atoms and the 2p orbital of the C atoms are hybridized, which is the source of the adsorption energies. Not surprisingly, G-SV-NiO has the most intense Ni 3d orbital and C 2p orbital hybridization.

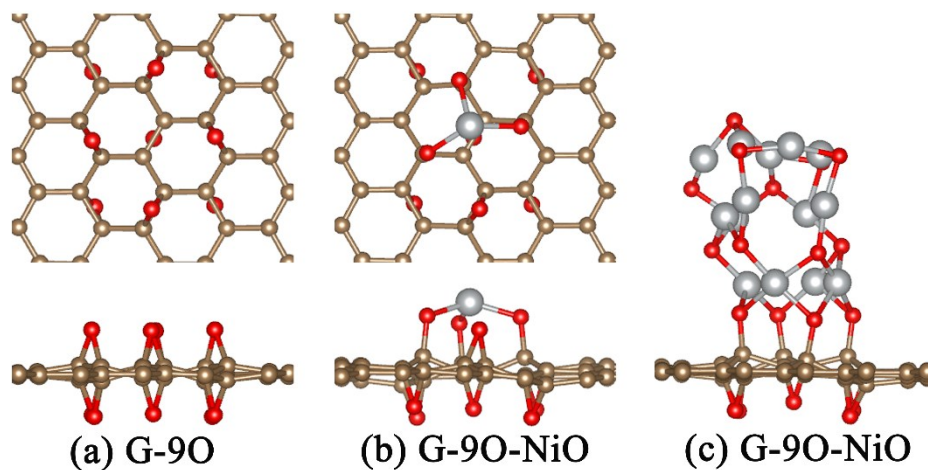


Fig. S10 Relaxed lattice structure of (a) G-9O: The graphene surface is locally loaded with 9 epoxy groups.⁶ (b) G-9O-Ni: Ni atoms are bonded to three epoxy groups on the substrate to form Ni-O-C bonds with the absorption energy of -3.88 eV. (c) G-9O-NiO: NiO clusters are attached to four epoxy groups on the substrate to form Ni-O-C bonds with the absorption energy of -5.26 eV.

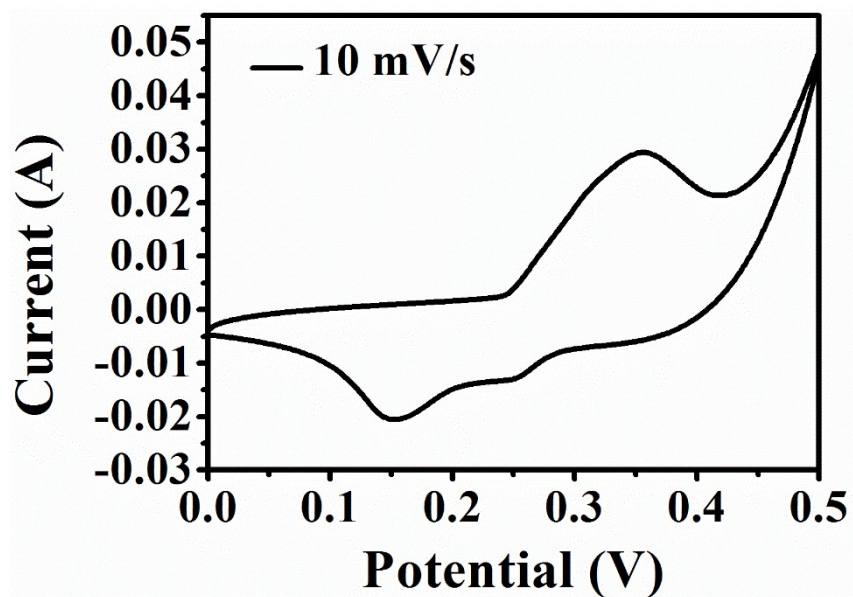


Fig. S11 The cyclic voltammetry curves of NiO NDs@rGO at 10 mV s⁻¹.

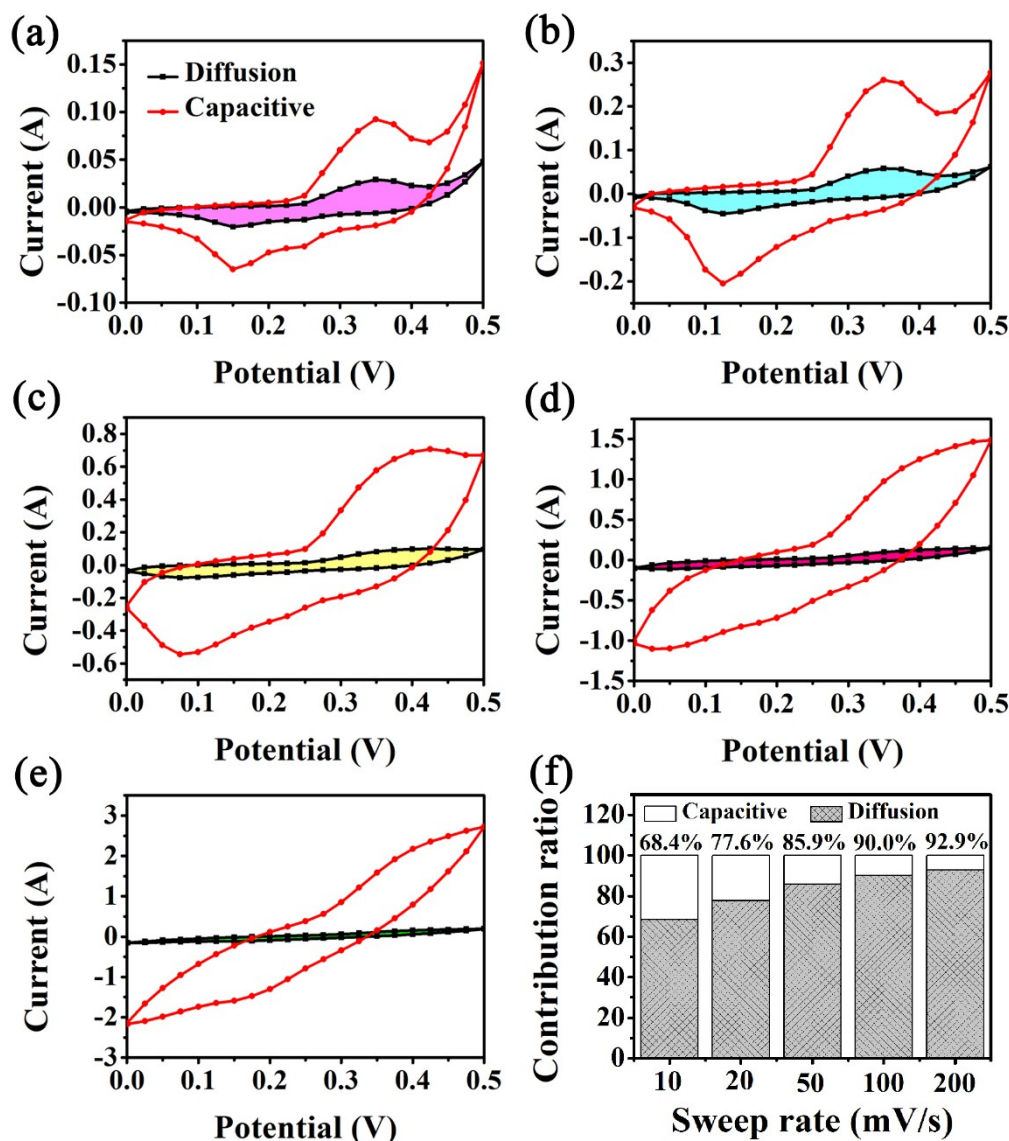


Fig. S12 Cyclic voltammetry of NiO NDs@rGO composite at (a) 10 mV s⁻¹, (b) 20 mV s⁻¹, (c) 50 mV s⁻¹, (d) 100 mV s⁻¹, (e) 200 mV s⁻¹, and (f) separation of capacitive charge and diffusion-controlled at different sweep rate. The shadow area represents the capacitive contribution.

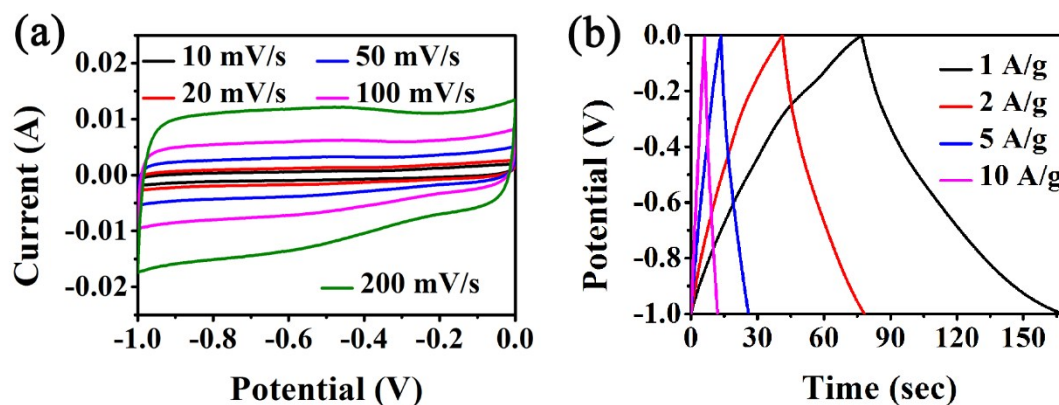
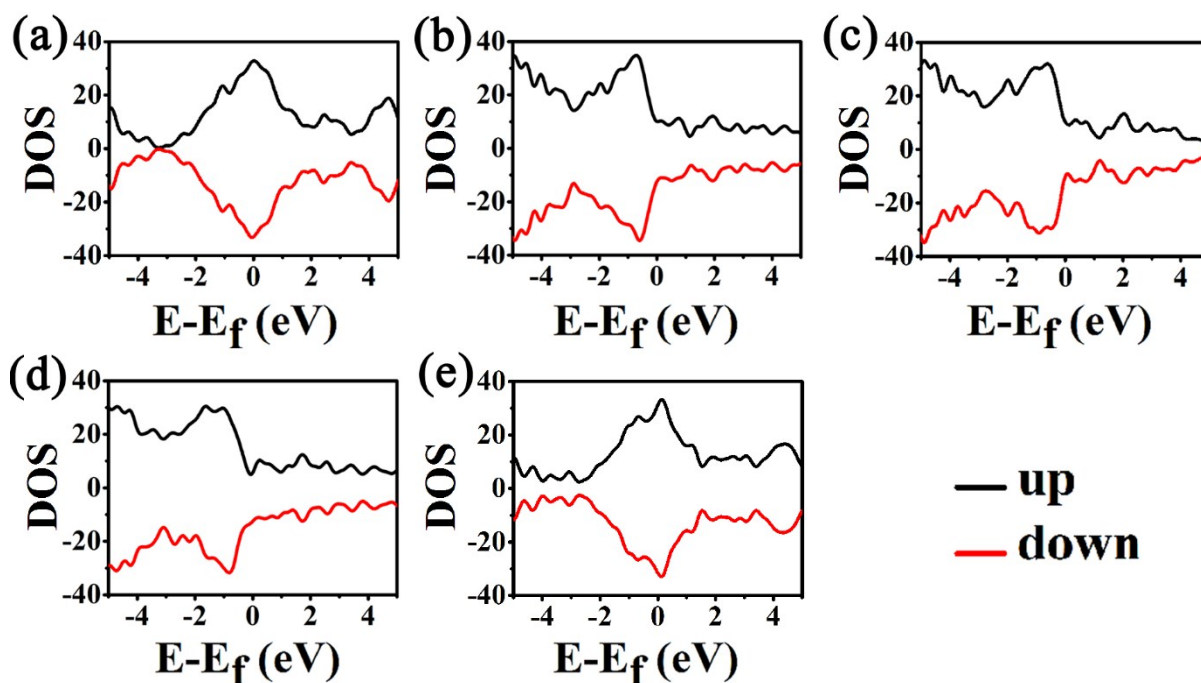


Fig. S13 The Electrochemical properties of pure rGO. (a) CV curves of rGO at various scan rates. (b) Charge-discharge curves at different current densities.

Table. S2 The comparison of the electrochemical performance of reported NiO/G composite in recent papers and our results.

NiO/G	Electrolyte potential range	Specific capacitance	Rate capability	Cycling stability	years
RGO-NiO	6 M KOH 0.05-0.55 V	576 F g ⁻¹ at 1 A g ⁻¹	70% at 10 A g ⁻¹	100% after 1100 cycles at 1 A g ⁻¹ .	2012 ⁷
NiO nanoflakes/graphene	6 M KOH 0-0.5 V	274 F g ⁻¹ at 1 A g ⁻¹	80% at 10 A g ⁻¹	100-120% after 1500 cycles at 5 A g ⁻¹	2013 ⁸
3D NiO-graphene	2 M KOH 0-0.45 V	651 F g ⁻¹ at 1 A g ⁻¹	46% at 20 A g ⁻¹	80% after 2000 cycles at 2 A g ⁻¹	2014 ⁹
3D NiO/UDG/NF	5 M KOH 0-0.4 V	425 F g ⁻¹ at 2 A g ⁻¹	70.6% at 10 A g ⁻¹	79% after 2000 cycles at 10 A/g	2014 ¹⁰
RG/NiO	5 M NaOH 0-0.8 V	617 F g ⁻¹ at 1 A g ⁻¹	—	94% after 5000 cycles at 1 A g ⁻¹ .	2014 ¹¹
Graphene/NiO Nanowires	6 M KOH 0-0.5 V	628 F g ⁻¹ at 1 A g ⁻¹	67.4% at 15 A g ⁻¹	82.4% after 3000 cycles at 1 A g ⁻¹	2014 ¹²
3D-RGNi	2 M KOH -0.1-0.35 V	1328 F g ⁻¹ at 1 A g ⁻¹	62% at 10 A g ⁻¹	87% after 2000 cycles at 2 A g ⁻¹	2015 ¹³
NiO nanoflake - 3D graphene	1 M NaOH 0-0.6 V	1829 F g ⁻¹ at 3 A g ⁻¹	55 % at 15 A g ⁻¹	85% after 5000 cycles at 15 A g ⁻¹	2015 ¹⁴
G@NiO nanosheet	2 M KOH 0-0.4 V	1073 C g ⁻¹ at 1 A g ⁻¹	59% at 20 A g ⁻¹	99% after 10000 cycles at 10 A g ⁻¹	2017 ¹⁵
NiO NDs@rGO	2 M KOH 0-0.35 V	1020.28 F g ⁻¹ at 1 A g ⁻¹	92% at 10 A g ⁻¹	78% after 2000 cycles at 5 A g ⁻¹	this work

**Fig. S14** The DOS of (a) G-NiO, (b) G-O-NiO, (c) G-OH-NiO, (d) G-SV-NiO, and (e) G-SW-NiO.

References

- 1 Ferrari, A. C.; Meyer, J. C.; Scardaci, V.; Casiraghi, C.; Lazzeri, M.; Mauri, F.; Piscanec, S.; Jiang, D.; Novoselov, K. S.; Roth, S.; Geim, Phys. Rev. Lett. 2006, 97, 187401–187404.
- 2 F. Banhart, J. Kotakoski and A. V. Krasheninnikov, *ACS Nano*, 2011, **5**, 26-41.
- 3 K. Suenaga, H. Wakabayashi, M. Koshino, Y. Sato, K. Urita and S. Iijima, *Nat. Nanotechnol.*, 2007, **2**, 358-360.
- 4 L. Shahriary and A. A. Athawale, *Int. J. Renew. Energy Environ. Eng*, 2014, **2**, 58-63.
- 5 A. Bagri, C. Mattevi, M. Acik, Y. J. Chabal, M. Chhowalla and V. B. Shenoy, *Nat. Chem.*, 2010, **2**, 581.
- 6 Ž. Šljivančanin, A. S. Milošević, Z. S. Popović and F. R. Vukajlović, *Carbon*, 2013, **54**, 482-488.
- 7 Y. Y. Yang, Z. A. Hu, Z. Y. Zhang, F. H. Zhang, Y. J. Zhang, P. J. Liang, H. Y. Zhang and H. Y. Wu, *Mater. Chem. Phys.*, 2012, **133**, 363-368.
- 8 Y. G. Zhu, G. S. Cao, C. Y. Sun, J. Xie, S. Y. Liu, T. J. Zhu, X. B. Zhao and H. Y. Yang, *RSC Adv.*, 2013, **3**, 19409-19415.
- 9 M. L. Huang, C. D. Gu, X. Ge, X. L. Wang and J. P. Tu, *J. Power Sources*, 2014, **259**, 98-105.
- 10 C. H. Wu, S. X. Deng, H. Wang, Y. X. Sun, J. B. Liu and H. Yan, *ACS Appl. Mater. Interfaces*, 2014, **6**, 1106.
- 11 Y. Chen, Z. Huang, H. Zhang, Y. Chen, Z. Cheng, Y. Zhong, Y. Ye and X. Lei, *Int. J. Hydrogen Energy*, 2014, **39**, 16171-16178.
- 12 D. T. Dam, X. Wang and J. M. Lee, *ACS Appl. Mater. Interfaces*, 2014, **6**, 8246.
- 13 N. B. Trung, T. V. Tam, D. K. Dang, K. F. Babu, E. J. Kim, J. Kim and W. M. Choi, *Chem. Eng. J.*, 2015, **264**, 603-609.
- 14 C. Wang, J. Xu, M. F. Yuen, J. Zhang, Y. Li, X. Chen and W. Zhang, *Adv. Funct. Mater.*, 2015, **24**, 6372-6380.
- 15 J. Lin, H. Jia, H. Liang, S. Chen, Y. Cai, J. Qi, C. Qu, J. Cao, W. Fei and J. Feng, *Adv. Sci.*, 2017, **5**, 1700687.